

# Dynamical instabilities of quasistatic crack propagation under thermal stress

Eran Bouchbinder,<sup>1</sup> H. George E. Hentschel,<sup>1,2</sup> and Itamar Procaccia<sup>1,3</sup>

<sup>1</sup>Department of Chemical Physics, The Weizmann Institute of Science, Rehovot 76100, Israel

<sup>2</sup>Physics Department, Emory University, Atlanta, Georgia 30322, USA

<sup>3</sup>Department of Physics, The Chinese University of Hong Kong, Shatin, Hong Kong

(Received 12 May 2003; published 3 September 2003)

We address the theory of quasistatic crack propagation in a strip of glass that is pulled from a hot oven towards a cold bath. This problem had been carefully studied in a number of experiments that offer a wealth of data to challenge the theory. We improve upon previous theoretical treatments in a number of ways. First, we offer a technical improvement of the discussion of the instability towards the creation of a straight crack. This improvement consists in employing Padé approximants to solve the relevant Wiener-Hopf factorization problem that is associated with this transition. Next we improve the discussion of the onset of oscillatory instability towards an undulating crack. We offer a way of considering the problem as a sum of solutions of a finite strip without a crack and an infinite medium with a crack. This allows us to present a closed form solution of the stress intensity factors in the vicinity of the oscillatory instability. Most importantly we develop a *dynamical* description of the actual trajectory in the regime of oscillatory crack. This theory is based on the dynamical law for crack propagation proposed by Hodgdon and Sethna. We show that this dynamical law results in a solution of the actual crack trajectory in post-critical conditions; we can compute from first principles the critical value of the control parameters, and the characteristics of the solution such as the wavelength of the oscillations. We present detailed comparison with experimental measurements without any free parameters. The comparison appears quite excellent. Finally we show that the dynamical law can be translated to an equation for the amplitude of the oscillatory crack; this equation predicts correctly the scaling exponents observed in experiments.

DOI: 10.1103/PhysRevE.68.036601

PACS number(s): 46.25.Hf, 62.20.Mk, 81.40.Np

## I. INTRODUCTION

In 1993 Yuse and Sano reported a simple experiment on fracture in glass [1] that nevertheless has attracted great attention from the fracture community. The experiment examined a strip of glass pulled at constant velocity  $v$  from an oven into water, cf. Fig. 1. At small enough velocity nothing happens. A first critical velocity heralds the onset of a straight crack, whereas exceeding a second critical velocity results in an oscillatory crack. Finally, at sufficiently high velocities the crack pattern exhibits multiple fractures and disorder. The reason for the high interest in this relatively simple experiment is, of course, that it offers a challenge for the theoretical description of fracture processes. Being essentially a “quasistatic” process, as the velocity  $v$  is very much smaller than the Rayleigh speed, the fracture process here is free of many of the complications arising in truly dynamic fracture [2]. Nevertheless, in the absence of a microscopic theory of the “process zone” (how materials actually break) even the dynamics of quasistatic crack propagation in brittle materials remains a debatable issue.

The lack of dynamical theory for the cracking process does not hinder the understanding of the onset of *straight* cracks in the above experiment. Indeed, already in the year following the original experimental observations, Marder set up the equations describing the effect of the temperature field on the elastic theory of the material, and presented a qualitative description of the onset of straight cracks [3]. From the quantitative point of view this treatment was lacking, in particular the fracture energy turned out to be strongly velocity dependent against physical intuition. The tools employed by

Marder did not allow however a correct prediction of the characteristics of oscillatory crack propagation. The next decisive theoretical step was taken by Adda-Bedia and Pomeau [4]. These authors not only reproduced Marder’s results for straight cracks, but also developed a successful criterion for the secondary instability to oscillatory cracks. They employed the universal form of the near-tip stress tensor field, i.e.,

$$\sigma_{ij}(r, \theta) = \frac{K_I}{\sqrt{2\pi r}} \Sigma_{ij}^I(\theta) + \frac{K_{II}}{\sqrt{2\pi r}} \Sigma_{ij}^{II}(\theta). \quad (1)$$

Here  $K_I$  and  $K_{II}$  are the “stress intensity factors” with respect to the opening and shear modes, whereas  $\Sigma_{ij}^I(\theta)$  and  $\Sigma_{ij}^{II}(\theta)$  are universal angular functions common to all configurations and loading conditions. Adda-Bedia and Pomeau

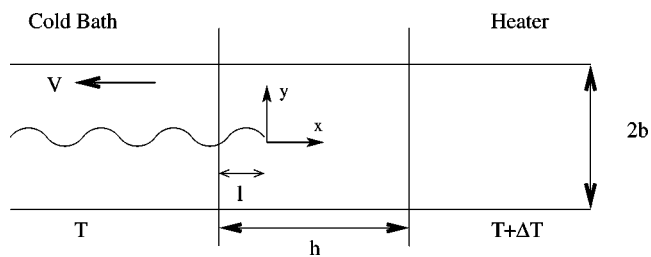


FIG. 1. Schematic representation of the experiment: a thin glass plate is pulled at a velocity  $v$  away from a heater into a cold bath. The control parameters are the temperature difference between the oven and the water  $\Delta T$ , the pulling velocity  $v$ , the spatial separation between the thermal baths  $h$ , and the width of the plate  $2b$ .

invoked the well-known and extensively used “principle of local symmetry” [6], which states that the path taken by a crack in brittle homogeneous isotropic material is such that the local stress field at the tip of the crack is of mode I type, annulling  $K_{II}$ . The considerations in Ref. [4] led to the conclusion that the appearance of a negative  $K_{II}$  for positive deviations from straight trajectory (or positive  $K_{II}$  for negative deviations) was tantamount to the onset of the oscillatory instability. Nevertheless, these authors did not offer a careful quantitative comparison against the experiments known at the time. Their prediction of the fracture energy and the wavelength of oscillations differed significantly from the experimental values.

In light of these results, we should explain at this point why do we feel that further theory is called for. First, we point out that “principle of local symmetry” is hardly a dynamical theory. It can predict an instability, but taken literally would only agree with a fracture path that has sharp kinks. It cannot be employed to predict the actual trajectory of a slowly moving crack when the latter is not straight. Second, since the theoretical works cited above there have been additional experimental studies of this very same problem [7–10], offering a wealth of data to challenge the theory, a challenge that had not been picked up by the theorists. Last, but not least, we feel that we can improve on a number of technical issues tackled by previous authors; these will be spelled out in the sequel, hopefully gratifying the diligent reader as we go along.

From the conceptual point of view we offer a point of departure from previous treatments by adopting a *dynamical* description of the crack development. In this we follow Hodgdon and Sethna [11] who have built upon the principle of local symmetry, using standard theoretical methods, to reach a dynamical law for crack propagation which is given by

$$\begin{aligned}\frac{\partial \mathbf{r}_{tip}}{\partial t} &= v \hat{\mathbf{t}}, \\ \frac{\delta \hat{\mathbf{t}}}{\delta t} &= -f K_{II} \hat{\mathbf{n}},\end{aligned}\quad (2)$$

where  $\hat{\mathbf{t}}$  and  $\hat{\mathbf{n}}$  are the tangent and the normal to the crack tip, respectively, and  $f > 0$  is a material function that we assume to be nearly independent of  $\hat{\mathbf{t}}$  and  $\hat{\mathbf{n}}$  in the quasistatic limit. This law predicts a *differentiable* crack path such that  $K_{II}$  is reduced. We will demonstrate that this law of motion provides us with predictions that are in excellent agreement with the characteristics of the crack trajectory in the oscillatory regime. We believe that this is the first context in which Eqs. (2) are compared against a challenging set of experimental data; the comparison appears quite favorable.

In Sec. II we discuss, facing the danger of being superfluous, the problem of the primary instability leading to a straight crack propagation once more. This instability had been correctly treated in Refs. [3,4], but we offer a technical improvement in the handling of the Wiener-Hopf factorization problem that is the basis of the solution. Using recent

mathematical advances [12] we use Padé approximants to significantly improve the treatment. Since the results of this improved treatment are relied upon in our solution of the oscillatory instability, we present the theory for the straight crack in some detail. Section III introduces the main results of our study in the context of the secondary instability to oscillatory cracks. Using the dynamical law Eq. (2) we show that as one crosses the second critical value of the parameters the solution of the equations changes its nature. We solve the equation near the onset of the oscillatory instability and calculate the critical values of the control parameters, the wavelength of oscillations, and the material function  $f$ . Although our criterion for the oscillatory instability is in agreement with Refs. [4,5] (which was based on the “principle of local symmetry”), we can go considerably further in describing the actual dynamics in the oscillatory regime. In particular we present a quantitative comparison with the experiments. Our handling of the oscillatory instability includes also a technical improvement on the analysis of Ref. [4]; the latter needed a separate Wiener-Hopf problem for every order in the amplitude of the perturbation. In our calculation we derive a new expression for  $K_{II}$  to leading order in the amplitude of the oscillations, an expression that requires a solution of only one Wiener-Hopf problem. This simplification is achieved by presenting a different way to decompose the straight crack problem into a singular and a nonsingular part and then using a classical result of Cotterell and Rice [13]. A crucial step in the calculation is the Wiener-Hopf factorization, for which we apply the method of solution based on Padé approximants [12]. Employing the dynamical law of crack-tip propagation we calculate the critical exponents for the transition and compare them with the experimental data. Section IV offers a summary and concluding remarks.

## II. THE STRAIGHT CRACK

### A. Preliminaries

By varying the experimental control parameters one varies the amount of elastic energy stored in the glass plate. One can choose various paths in parameter space; in this work we adopt the scheme of Ref. [9], fixing the values of  $\Delta T$ ,  $h$ , and  $v$ . The growth state depends then on the plate’s width  $2b$ : for small enough values of the width a seeded crack does not grow; for a width greater than a critical value  $L_c$ , a crack, whose tip penetrates a length  $\ell$  away from the cold bath, moves at a velocity  $-v$ . This crack is stationary in the laboratory frame of reference and is stable as long as the width is smaller than another critical value  $L_{osc}$ . Above this value the crack becomes unstable and exhibits an oscillatory lateral motion with a well-defined amplitude and wavelength, still traveling at a velocity  $-v$ . As the width is further increased the propagation becomes less and less regular.

The no crack–straight crack propagation transition is well understood and the agreement with the experimental data is favorable [7]. In this case the propagation is pure mode I and the transition is governed by the following Irwin relation:

$$\frac{K_I^2}{E} = \Gamma, \quad (3)$$

where  $\Gamma$  is the fracture energy which is a material property and  $E$  is Young's modulus. In this section we address again this problem and describe the formal solution. The merit of our treatment will be in providing a detailed scheme for performing the Wiener-Hopf factorization in a different way.

### B. The formulation of the problem

Imagine the glass plate as in Fig. 1 with a straight crack penetrating into the glass from the water side. We choose a coordinate system such that  $x=0$  is at the crack tip (marking the water level at  $x=-\ell$ , where  $\ell$  is the penetration depth of the straight crack). The  $y$  coordinate spans the interval  $[-b, b]$ . The condition for mechanical equilibrium under plane stress conditions caused by a nonuniform temperature field reads

$$\nabla^2 \nabla^2 \chi(x, y) = -E\alpha_T \nabla^2 T(x), \quad (4)$$

where  $\alpha_T$  is the thermal expansion coefficient and  $\chi$  is the Airy potential which is related to the stress tensor by

$$\sigma_{xx} = \frac{\partial^2 \chi}{\partial y^2}, \quad \sigma_{yy} = \frac{\partial^2 \chi}{\partial x^2}, \quad \sigma_{xy} = -\frac{\partial^2 \chi}{\partial x \partial y}. \quad (5)$$

Using the symmetry of the problem we state the boundary conditions as follows:

$$\sigma_{yy}(x, \pm b) = \sigma_{xy}(x, \pm b) = \sigma_{xy}(x, 0) = 0, \quad (6)$$

$$\sigma_{yy}(x, 0) = 0 \quad \text{for } x \leq 0, \quad u_y(x, 0) = 0 \quad \text{for } x \geq 0. \quad (7)$$

Fourier transforming Eq. (4) in the  $x$  direction and focusing on the upper half plate one obtains [3] the following Wiener-Hopf equation [14]:

$$\hat{\sigma}_{yy}(k, 0) = -F(k)\hat{u}_y(k, 0) + D_\ell(k) \quad (8)$$

with

$$F(k) = Ek \frac{\sinh^2(kb) - kb^2}{\sinh(2kb) + 2kb}, \quad (9)$$

$$D_\ell(k) = 2E\alpha_T \hat{T}_\ell(k) \frac{[1 - \cosh(kb)][\sinh(kb) - kb]}{\sinh(2kb) + 2kb}, \quad (10)$$

where one still has to obey the boundary conditions of Eq. (7). Note that the subscript  $\ell$  denotes the transformation  $x \rightarrow x + \ell$  in the temperature field such that the origin of the coordinates system is at the tip of the crack. For convenience, from now on, we rescale all lengths in the problem by the half-width  $b$ .

Writing  $F(k) = F^-(k)/F^+(k)$ , where  $F^-(k)$  has neither zeros nor singularities for  $\text{Im}(k) < 0$ , and  $F^+(k)$  has neither zeros nor singularities for  $\text{Im}(k) > 0$ , the Wiener-Hopf method [14] results in

$$\hat{u}_y(k, 0) = \frac{1}{F^-(k)} \int_{-\infty}^0 d\tilde{x} \left[ \int_{-\infty}^{\infty} \frac{d\tilde{k}}{2\pi} D_\ell(\tilde{k}) F^+(\tilde{k}) e^{-i\tilde{k}\tilde{x}} \right] e^{ik\tilde{x}}. \quad (11)$$

From this solution one can extract [4] the mode I stress intensity factor introduced in Eq. (1),

$$K_I(\Delta T, v, b, h) = \int_{-\infty}^{\infty} \frac{dk}{2\pi} D_\ell(k) F^+(k). \quad (12)$$

Note that if the fracture energy  $\Gamma$  is known then the mode I stress intensity factor characterizes completely the no crack–straight crack transition.  $K_I$  is a positive quantity and is different from zero, as a function of  $\ell$ , only on a scale of the order of  $b$ . To calculate this quantity we need first to solve for the temperature field and second to provide a method for accomplishing the Wiener-Hopf factorization.

### C. The temperature field

The nonuniform temperature field induces the stress field in the elastic plate. In this section we solve for the temperature field and study its properties. For simplicity, we set the zero of the coordinates system at the cooling front level to avoid  $\ell$  dependence which is unnecessary in the present context. For later calculations we will use the aforementioned transformation to put back the  $\ell$  dependence.

In the frame of reference of the plate the temperature field obeys the heat equation

$$\frac{\partial T}{\partial t} = D \nabla^2 T \quad (13)$$

with the boundary conditions

$$\vec{\nabla} T \cdot \vec{n} = 0,$$

$$T(x=0) = T,$$

$$T(x=h) = T + \Delta T. \quad (14)$$

Here  $D \approx 0.47 \text{ mm}^2/\text{sec}$  is the diffusion coefficient of the glass,  $h$  is the distance between the cold bath and the heater, and  $\vec{n}$  is the unit vector normal to the boundary of the domain.

This equation can be simplified for the straight crack configuration, for which there is no  $y$  dependence, by looking for a stationary solution in the laboratory frame of reference, of the form  $T(x - vt)$ . This solution obeys the stationary diffusion equation

$$\nabla^2 T + \frac{1}{d_{th}} \frac{\partial T}{\partial x} = 0, \quad (15)$$

where  $d_{th} = D/v$  is the thermal diffusion length. The exact solution of this equation is

$$T(x) = \Delta T \left[ \frac{1 - e^{-x/d_{th}}}{1 - e^{-h/d_{th}}} \theta(x) \theta(h-x) + \theta(x-h) \right]. \quad (16)$$

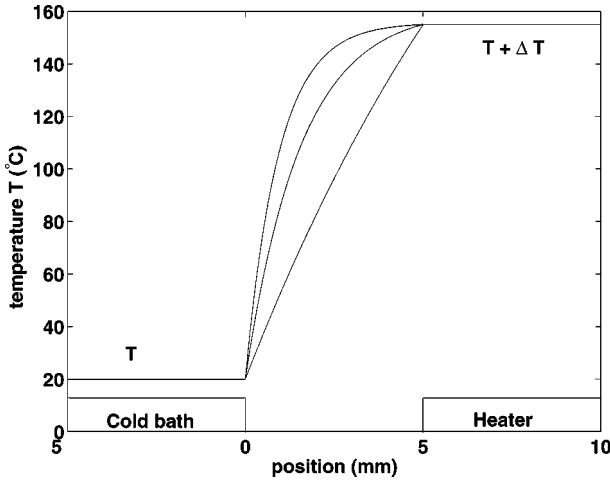


FIG. 2. The calculated temperature distribution inside the glass plate. We can identify two distinct regimes—the diffusive regime at low velocities ( $v=0.05$  mm/sec in the lower curve) and the advective regime at higher velocities ( $v=0.3$  mm/sec, and  $v=0.5$  mm/sec in the upper two curves). These curves should be compared with the measured temperature field in Ref. [9].

We can identify two distinct regimes, as shown in Fig. 2. The first one, at low velocities, is the diffusive regime, in which the temperature field is controlled by the spatial separation of the thermal baths  $h$ . The second one, at higher velocities, is the advective regime, in which the temperature field is controlled by the thermal diffusion length  $d_{th}$ . Actually, there is a third regime, at still higher velocities, in which the temperature field is controlled by the thickness of the plate. Note that we assumed that the temperature is uniform along this dimension and therefore the breakdown of this assumption in this regime leads to a three-dimensional problem, which is outside the scope of our two-dimensional model.

The temperature field enters the problem through the term  $-E\alpha_T\nabla^2 T(x)$  of the inhomogeneous Bi-Laplace equation. This term is sensitive only to variations of the temperature gradient, i.e., to the curvature of the thermal field. In Eq. (16) we considered a finite spatial separation between the thermal baths, but assumed perfect thermal baths, an assumption that leads to a discontinuity of the gradient near the baths. This discontinuity results in incorrect estimates of the stress field; since at low velocities (see Fig. 2) the only gradient variations are in these regions, we cannot expect a very good quantitative agreement with the experiment for low velocities. At higher velocities, there is a significant curvature inside the glass, so we expect a better quantitative agreement with the experiment. In Ref. [9] the temperature field was measured and found to vary smoothly near the baths due to the finite impedances of the baths. In the absence of the experimental data of the measured temperature field we will use the ideal baths approximation.

#### D. The Wiener-Hopf factorization

The crucial element in the solution is the Wiener-Hopf factorization of the known kernel  $F(k)$ . Generally it is not

possible to find an *exact* factorization, so one tries an approximant  $\tilde{F}(k) \approx F(k)$  that can be exactly factorized. This can be made rigorous following a recently proven theorem [12] which establishes the closeness of the product factors of  $\tilde{F}(k)$  to those of  $F(k)$  in their region of regularity if  $\tilde{F}(k) \approx F(k)$  for all  $k \in D$ , where  $D$  is the strip of analyticity of  $F(k)$ . A commonly followed first step in finding  $\tilde{F}(k)$  is to examine the behavior of  $F(k)$  near zero and  $\pm\infty$ ,

$$F(k) \rightarrow \pm \frac{k}{2} \quad \text{as } k \rightarrow \pm\infty, \quad (17)$$

$$F(k) \rightarrow \frac{k^4}{12} \quad \text{as } k \rightarrow \pm 0. \quad (18)$$

A standard approach to finding a good factorization is then to seek a function  $\phi(k)$  that reproduces the asymptotic behavior of  $F(k)$  and to correct it by a ratio of two polynomials

$$\tilde{F}(k) = \phi(k) \frac{k^4 + \alpha k^2 + \beta}{k^4 + \gamma k^2 + \beta}, \quad (19)$$

where, for example,

$$\phi(k) = \frac{k^4}{\sqrt{4k^6 + 144}}, \quad (20)$$

and  $\alpha, \beta, \gamma$  are free parameters that should be chosen as to best fit  $\tilde{F}(k)$  to  $F(k)$ . In principle, one can use higher order polynomial ratio to achieve greater accuracy. The disadvantage of this approach is that the positions of the poles and zeros are not well controlled and that the convergence behavior of the process is not clear.

In our work we follow a new method developed in Ref. [12]. In the heart of this approach lies the use of Padé approximants. An  $[N/M]$  approximant of  $F(k)$  is written as

$$\tilde{F}(k) \approx \frac{P_N(k)}{Q_M(k)}, \quad (21)$$

where

$$P_N(k) = a_0 + a_1 k + a_2 k^2 + \dots + a_N k^N, \quad (22)$$

$$Q_M(k) = 1 + b_1 k + b_2 k^2 + \dots + b_M k^M. \quad (23)$$

The coefficients  $a_n, b_n$  are determined from the Taylor-series expansion of  $F(k)$  at any regular point. Let us take the expansion point to be  $k=0$ , so

$$F(k) = \sum_{n=0}^{\infty} c_n k^n, \quad (24)$$

where  $c_n$  are known. In order to solve for the unknown coefficients one should set

$$\frac{P_N(k)}{Q_M(k)} + O(k^{N+M+1}) = \sum_{n=0}^{\infty} c_n k^n \quad (25)$$

to obtain a set of linear equations [12]. In this method one approximates directly the factorization and the process is completely algorithmic. Note that since in practice one uses the truncated series of  $F(k)$  it is not possible to approximate directly the product factors for arbitrary large  $k$ 's. In order to overcome this difficulty we should find the asymptotic form of the factorization and use it as a boundary condition for the Padé approximants. The asymptotic factorization is found by noticing that the zeros and poles of  $F(k)$ , which are, respectively, the solutions of the equations

$$\sinh^2(w_n) - w_n^2 = 0, \quad (26)$$

$$\sinh(2z_n) - 2z_n = 0 \quad (27)$$

have the property that if, for example,  $w_n$  is a zero of  $F(k)$  then  $\bar{w}_n$ ,  $-w_n$  and  $-\bar{w}_n$  are also zeros. The same holds for the poles. Therefore, considering the solutions of Eqs. (26) and (27) only in the first quadrant, we obtain

$$F(k) = \frac{k^4 \prod_{n=1}^{\infty} \left(1 - \frac{k}{w_n}\right) \left(1 + \frac{k}{w_n}\right) \left(1 - \frac{k}{\bar{w}_n}\right) \left(1 + \frac{k}{\bar{w}_n}\right)}{12 \prod_{n=1}^{\infty} \left(1 - \frac{k}{z_n}\right) \left(1 + \frac{k}{z_n}\right) \left(1 - \frac{k}{\bar{z}_n}\right) \left(1 + \frac{k}{\bar{z}_n}\right)}. \quad (28)$$

From here it follows that

$$F^-(k) = \frac{k^2 \prod_{n=1}^{\infty} \left(1 - \frac{k}{w_n}\right) \left(1 + \frac{k}{w_n}\right)}{\sqrt{12} \prod_{n=1}^{\infty} \left(1 - \frac{k}{z_n}\right) \left(1 + \frac{k}{z_n}\right)} = \frac{1}{F^+(-k)}. \quad (29)$$

Using this relation and the asymptotic relation of Eq. (17) we conclude that the asymptotic factorization is

$$F^+(k) \rightarrow \sqrt{\frac{2}{-ik}}, \quad F^-(k) \rightarrow \sqrt{\frac{ik}{2}}. \quad (30)$$

We should choose the Padé approximants to match these asymptotic forms. This is achieved by squaring the original kernel  $F(k)$ , to obtain an even function of  $k$  that behaves as  $k^2$  as  $|k| \rightarrow \infty$ . Hence, we can derive an  $[(N+2)/N]$  Padé approximation

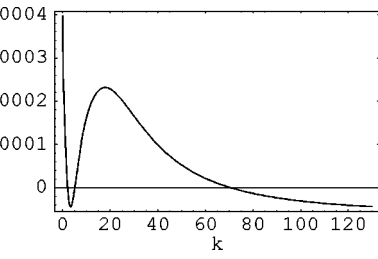
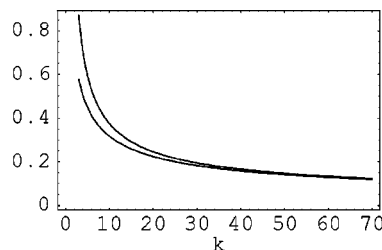
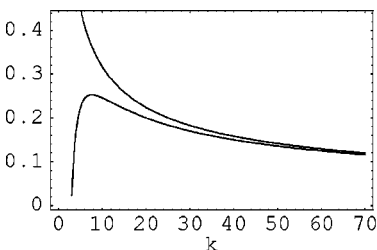


FIG. 3. The relative error,  $[F^-(k)/F^+(k) - F(k)]/F(k)$ , as a function of  $k$ .

$$F^2(k) \approx \frac{P_{N+2}(k)}{Q_N(k)}, \quad (31)$$

with  $N$  even. This approximation contains  $N+2$  zeros and  $N$  poles which become, after taking the square root,  $N-1$  branch points in the upper half-plane and  $N-1$  branch points in the lower half-plane. The relative error,  $(F^-(k)/[F^+(k) - F(k)])/F(k)$ , for  $N=28$  is shown in Fig. 3. The asymptotic matching of  $F^+(k)$  to  $\sqrt{2/(-ik)}$  is shown in Fig. 4.

### E. The determination of the fracture energy $\Gamma$

In Sec. III we develop a theory for the oscillatory instability and compare it with the experimental results. A crucial parameter in that theory, as here, is the fracture energy  $\Gamma$ . We can extract the fracture energy from the experimental threshold for propagation, cf. Eq. (3). The relevant measurement was reported in Ref. [7] in which a linear elastic model identical to ours was used to extract the fracture energy.  $\Gamma$  was chosen to best fit the experimental data of the onset of the straight crack propagation. It was found that  $\Gamma$  depends weakly on the velocity when the idealized thermal profile was employed;  $\Gamma$  turned out velocity independent for the actual thermal profile measured in the experiment. Since we do not have the experimental data for the thermal profile we will use, for consistency, a typical value of the former, i.e.,  $\Gamma \approx 3.75$  J/m<sup>2</sup>. This value should be compared to Fig. 5 in Ref. [7].

## III. THE STRAIGHT TO OSCILLATORY CRACK TRANSITION

Solving a dynamic fracture problem in the quasistatic limit consists of (i) solving the equilibrium equations for the stress field together with a given set of boundary conditions at the sample boundaries and on the (*a priori* unknown and evolving) crack boundary and (ii) employing a dynamical principle to evolve the crack. A proper solution determines

FIG. 4. The real (left-hand panel) and imaginary (right-hand panel) parts of  $F^+(k)$  (lower curve in both panels) compared to the real and imaginary parts of  $\sqrt{2/(-ik)}$ , as a function of  $k$ .

the correct shape of the crack as a function of time. Clearly, the predictions of the employed crack growth law should be consistent with the experimental observations. In this section we use the dynamical law in Eq. (2) to study the straight to oscillatory crack transition.

Rewriting the tangential and normal unit vectors at the tip of the crack in terms of the angle  $\theta$  that the tangential unit vector makes with the  $x$  axis, we obtain

$$\begin{aligned}\hat{t} &= \hat{x} \cos \theta + \hat{y} \sin \theta, \\ \hat{n} &= -\hat{x} \sin \theta + \hat{y} \cos \theta,\end{aligned}\quad (32)$$

which, upon substitution into Eq. (2), leads to

$$\frac{\partial \theta}{\partial t} = -fK_{II}. \quad (33)$$

This equation predicts that as long as  $K_{II}=0$ , the crack will propagate in a straight line. Nevertheless, in any real material there exist intrinsic instabilities, due to imperfections of the material and the loading conditions, which produce a small random  $K_{II} \neq 0$ . We are now facing two distinct questions: Under what conditions, in terms of the control parameters  $\Delta T$ ,  $h$ ,  $v$ , and  $2b$ , does straight crack propagation become unstable? Once the straight crack propagation becomes unstable, what is the stable stationary path that it follows?

The criterion of stability arises naturally from the dynamical equation. If  $\theta$  and  $K_{II}$  have the same sign, with  $f > 0$ , then  $\partial \theta / \partial t$  has the opposite sign and  $|\theta|$  decreases, which means that a small perturbation decays. By the same argument, for  $\theta$  and  $K_{II}$  having the opposite sign a small perturbation grows. This criterion is identical to that suggested in Refs. [4,5].

The question of the future evolution of the crack, once the instability threshold is reached, should be answered by solving the dynamical equation just above the onset of the instability. Guided by the experimental observation that the shape of the crack just above the onset of the oscillatory instability is a pure sine function, we introduce a smooth deviation from a straight crack path

$$y(x,t) \approx A \sin[w(x+vt)] + O(A^3) \quad \text{for } x \leq 0. \quad (34)$$

This assumption serves two roles: first, it represents a single mode component, corresponding to a wave number  $w$ , in the linear decomposition of a small random perturbation on top of the straight crack and will enable us, for  $t=0$ , to analyze its stability; second, it is an ansatz for the solution of the dynamical equation just above the onset of instability. Note that  $y(x,t)$  satisfies  $|y(x,t)| \ll 1$  and  $|y'(x,t)| \ll 1$ .

In this section we will study the stability of the straight crack as well as the time evolution of the crack after the onset of instability by analyzing the dynamical model of Eq. (33). The stability is studied by applying the stability criterion derived above for which an expression of  $K_{II}$  to leading order in the perturbation amplitude is needed. We derive this expression by introducing an auxiliary problem, the so-called decomposition problem, whose effective solution enables

one to significantly simplify the derivation. The critical point is calculated by solving the set of equations governing the transition. The time evolution of the crack just above the critical point is studied by directly solving the equations of motion for the tip of the crack.

### A. The decomposition problem

In order to study the stability of the straight crack to small perturbations we arbitrarily choose  $t=0$  in Eq. (34). This choice will be shown later to be legitimate. We are interested first in finding an expression for  $K_{II}$  to leading order in the amplitude of the perturbation. We begin by formulating an auxiliary problem. The presence of a crack, which is usually modeled as a mathematical branch cut, introduces the famous square-root singularity of the stress field near the tip of the crack. We want to represent our problem as a sum of two parts. The first part contains no singularity, implying that it is crack free, but it includes the geometry of the problem and the thermal field. The second part contains the singularity, implying that there is a crack with a given load on it, but the domain is infinite. The nonsingular part is chosen such that it reproduces the required boundary conditions on the plate's edges and on the crack.

Once we obtain the load on the semi-infinite straight crack in an infinite medium we can apply the classical result of Cotterell and Rice for slightly curved cracks [13]. The mathematical formulation of this decomposition problem leads to a set of integro-differential equations whose complexity may cast doubt on the usefulness of the whole procedure [16]. In what follows we will show how to avoid these mathematical difficulties and effectively solve the problem.

To see that the solution is almost at hand, suppose for a moment that we succeeded to solve the problem in this way for a straight crack and for a given set of the control parameters. The load on a straight crack in *an infinite domain*, which is a fictitious quantity, must be a pure mode I load by symmetry. We denote it as  $\sigma_{yy}^f(x, y=0; \ell)$ , where we marked explicitly the parametric dependence on  $\ell$ . The mode I stress intensity factor is given by [15]

$$K_I(\ell) = \sqrt{\frac{2}{\pi}} \int_{-\infty}^0 \frac{dx \sigma_{yy}^f(x, y=0; \ell)}{\sqrt{-x}}. \quad (35)$$

Introduce now the  $x$ -Fourier transform of  $\sigma_{yy}^f(x, y=0; \ell)$ , denoted as  $\hat{\sigma}_{yy}^f(k, y=0; \ell)$ . With this object in mind we rewrite Eq. (35) as

$$K_I(\ell) = \int_{-\infty}^{\infty} \frac{dk}{2\pi} \hat{\sigma}_{yy}^f(k, y=0; \ell) \left[ \sqrt{\frac{2}{\pi}} \int_{-\infty}^0 \frac{dx e^{-ikx}}{\sqrt{-x}} \right]. \quad (36)$$

On the other hand, we have calculated the same quantity using the Wiener-Hopf technique [see Eq. (12)]:

$$K_I(\ell) = \int_{-\infty}^{\infty} \frac{dk}{2\pi} D_0(k) e^{-ik\ell} F^+(k). \quad (37)$$

These two expressions for  $K_I(\ell)$ , though derived through completely different mathematical procedures, should be identical functions of  $\ell$ . The  $\ell$  dependence of the second expression is given by the phase factor  $e^{-ik\ell}$  which immediately implies that  $\hat{\sigma}_{yy}^f(k, y=0; \ell) = \tilde{\sigma}_{yy}(k, y=0) e^{-ik\ell}$ . We conclude, by the uniqueness of the Fourier transform, that

$$\tilde{\sigma}_{yy}(k, y=0) = \frac{D_0(k)F^+(k)}{\left[ \sqrt{\frac{2}{\pi}} \int_{-\infty}^0 \frac{dx e^{-ikx}}{\sqrt{-x}} \right]} = \frac{D_0(k)F^+(k)}{\sqrt{\frac{2}{-ik}}}, \quad (38)$$

which effectively solves the auxiliary problem.

Hence, we have shown how one can use the Wiener-Hopf solution for a traction-free straight crack in a finite configuration in order to find the effective load on a straight crack in an infinite configuration via the solution of the decomposition problem. We reiterate that this load is a fictitious tension on a crack in an infinite domain corresponding to a traction-free situation in a finite domain. The solution of this auxiliary problem will enable us later on to use the powerful tool of the complex potential method that is most suitable for an infinite domain problems. Other theoretical treatments that were unable to solve this problem led to incorrect predictions [16].

We comment that the approach described in this section is equally valid for general loading conditions, including mode II. The generalization is straightforward, but is not needed for the present problem.

### B. The critical point

The calculation now is straightforward. Let us select a local coordinate system  $\{r, \theta\}$  at every point on the crack, with  $r$  being the distance from the point and  $\theta$  being the angle, starting with  $\theta=0$  for the tangent. In such coordinates the normal opening stress  $T_n(x, y(x, t)) \equiv \sigma_{\theta\theta}(x, y(x, t))$  and the tangential shearing stress  $T_t(x, y(x, t)) \equiv \sigma_{r,\theta}(x, y(x, t))$ . Using the load  $\sigma_{yy}^f$  we can find these stress components for any small deviation  $y(x, t)$  from the straight crack. Applying these loads to the classical result of Cotterell and Rice [13], with  $t=0$ , we obtain the following expressions for  $K_I$  and  $K_{II}$  to leading order in  $A$  (see the Appendix):

$$K_I = \sqrt{\frac{2}{\pi}} \int_{-\infty}^0 \frac{dx \hat{\sigma}_{yy}^f(k, y=0; \ell)}{\sqrt{-x}} + O(A^2),$$

$$K_{II}(A, w, t=0) = - \sqrt{\frac{2}{\pi}} \int_{-\infty}^0 \frac{dx [A \sin(wx) \hat{\sigma}_{yy}^f(k, y=0; \ell)]}{(-x)^{3/2}} + \frac{1}{2} A w K_I + O(A^3). \quad (39)$$

This result shows that only  $K_{II}$  is changed to first order in the amplitude of the perturbation. The expression for  $K_{II}$  has the general form derived in Ref. [5]. It is the sum of two competitive terms which the authors of Ref. [5] refer to as a

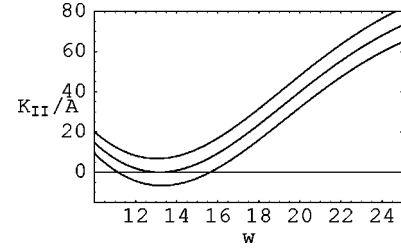


FIG. 5.  $K_{II}/A$  vs the dimensionless wave number  $w$ . For fixed  $\Delta T$ ,  $v$ , and  $h$ , the curves from top down show the increasing of the stored elastic energy via the increasing of the width of the plate. It is clear that there is a critical width for which  $K_{II}(w)=0$ .

“physical” shear stress which is a destabilizing term (the first term), and as a “geometric” shear stress, which is a stabilizing term (the second term). We expect to find a range of the control parameters for which for every  $w \neq 0$  the second term dominates the first, leading to  $K_{II} > 0$ , which implies a stable straight crack propagation. Thus, our stability criterion states that the transition between straight and oscillatory crack propagation occurs when there exist  $A, w \neq 0$  such that  $K_{II}(A, w, t=0) = 0$ . One concludes that the straight crack to oscillatory crack transition is governed by the following set of equations:

$$\frac{K_I^2(b, \ell) + K_{II}^2(b, \ell, w)}{E} \simeq \frac{K_I^2(b, \ell)}{E} = \Gamma,$$

$$K_{II}(b, \ell, w) = 0,$$

$$\frac{\partial K_{II}(b, \ell, w)}{\partial w} = 0, \quad (40)$$

where we made explicit the dependence on  $b$ ,  $\ell$ , and  $w$ .

The first equation is the Irwin’s relation that expresses the energy balance between the elastic energy flow to the tip of the crack and the fracture energy needed to create a new crack surface. This fracture energy is a parameter of our model; in previous applications this parameter was optimized for agreement with experiments [7]. We cannot afford such luxury since we have determined already the parameter in Sec. II E. Therefore in our comparison with experiments the theory is truly challenged, and the agreement will be shown to be very satisfactory.

The second and third equations express the stability threshold. In order to characterize quantitatively this transition we adopt the experimental scheme of Ref. [9], in which  $\Delta T$  and  $h$  are kept fixed and for a given  $v$  the critical width for the the onset of oscillations,  $L_{osc}$ , is found. Figure 5 shows a typical situation in which  $K_{II}/A$  is plotted as a function of  $w$  for different values of the width  $2b$  at constant  $\Delta T$ ,  $v$ , and  $h$ . It is shown that as one increases the width a solution for the equation  $K_{II}(A, w, t=0) = 0$  appears.

We solved the above set of equations graphically by the following procedure. We fixed  $\Delta T = 135^\circ\text{C}$  and  $h = 5$  mm and for each velocity we changed  $b$  until we converged to the solution. Note that first one has to solve the first equation for  $\ell$ . Figure 6 shows the critical width for oscillations

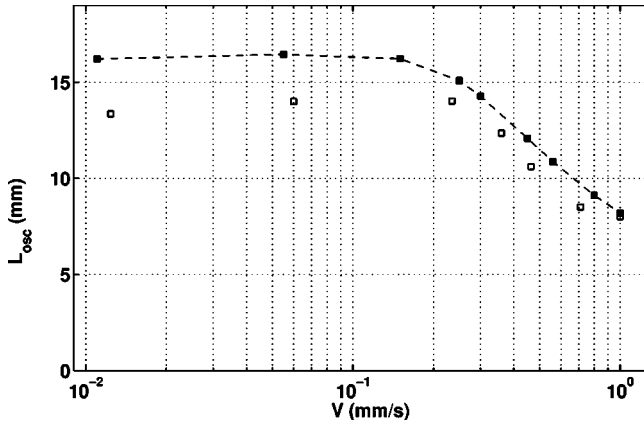


FIG. 6. The critical width for oscillations  $L_{\text{osc}}=2b_{\text{osc}}$  vs the driving velocity  $v$  for  $\Delta T=135^\circ\text{C}$  and  $h=5$  mm. We did not calculate these quantities for still higher velocities since this regime is controlled by three-dimensional effects which are outside the scope of our theory. The theoretical values are connected by the dashed line that was added as a guide for the eye. The experimental values that are represented by the unfilled squares were extracted from Fig. 15 in Ref. [9]. The deviation of  $L_{\text{osc}}$  from the measured data is due to its high sensitivity to the fine details of the temperature field, which we approximated, in the absence of the measured one, using the ideal baths assumption. It is clear, as predicted in Sec. II C, that the agreement with the experiment is much better within the advective regime than within the diffusive regime.

$L_{\text{osc}}=2b_{\text{osc}}$  as a function of the driving velocity  $v$ . The experimental data reported in Ref. [9] have been added for comparison.

The deviation of  $L_{\text{osc}}$  from the measured data is due to its high sensitivity to the fine details of the temperature field, which we approximated, in the absence of the measured one, using the ideal baths assumption. Nevertheless, as predicted

in Sec. II C, the agreement with the experiment is much better within the advective regime, in which the temperature field is controlled by  $d_{th}$ , than within the diffusive regime, in which the temperature field is controlled by  $h$ . Our solution here yields also the wave number of the unstable mode. In Ref. [5] this wave number was identified with the wave number of the actual trajectory in the post-critical conditions without further discussion. We find this unsatisfactory; whether or not this wave number will be observed in the actual crack trajectory also in post-critical conditions depends on the dynamics. If the “fastest growing mode” becomes stabilized by the nonlinear terms, then this wave number would be observed. To assess this issue we must turn next to the weakly nonlinear theory in the post-critical regime.

### C. The postcritical time evolution of the crack

Crack propagation laws used in the literature so far were unable to predict analytically nontrivial trajectories left behind a crack tip. The set of well-controlled experiments described here offers a challenge to any dynamical law, especially near the critical point where the crack exhibits a lateral oscillatory motion with a well-defined wavelength and amplitude. In this section we will show that the adopted dynamical law meets that challenge. The stationary stable path of the crack just above the onset of the oscillatory instability is determined by the solution of the dynamical equation near the transition. Noting that under our assumptions  $\theta \approx y'(0,t)$ , we obtain

$$\frac{\partial y'(0,t)}{\partial t} = -fK_{\text{II}}(A,w,t) + O(A^3). \quad (41)$$

Deriving the time dependent expression for  $K_{\text{II}}$  (see the Appendix) and substituting our ansatz (34), Eq. (41) becomes

$$\frac{Aw^2v}{f} \sin(wvt) = \sqrt{\frac{2}{\pi}} \int_{-\infty}^0 \frac{dx \{2A \sin[w(x+vt)] \sigma_{yy}^f(x,y=0;\ell)\}' - A \sin(wvt) \sigma_{yy}^f(x,y=0;\ell)}{\sqrt{-x}} + \frac{1}{2} Aw \cos(wvt) K_{\text{I}}. \quad (42)$$

This equation has a trivial solution, i.e.,  $A=0$ , which is the straight crack. An explicit calculation with  $A \neq 0$  determines that the right-hand side (RHS) of this equation is a pure sine function. Thus our ansatz (34) can be an actual solution only if we can choose the control parameters such as to set the phase of the sine function to zero at  $t=0$  (cf. the LHS). We see that this is possible with  $K_{\text{II}}(A,w,t=0)=0$  which is exactly what was calculated above in the context of linear stability analysis. Thus if this condition can be met, (and if  $A$  remains small above the critical point, cf. Sec. III D) we can indeed identify the aforementioned wave number as the wave number of the oscillations in the close vicinity of the critical point. We conclude that the equation of motion (33) is consistent with a pure sinusoidal trajectory,

which is an *exact solution of the post-critical* dynamics. This is in good agreement with the experimental observations. This result also shows that the arbitrary choice  $t=0$  in the linear stability analysis is legitimate since one has to fix the phase only at one time point.

Figure 7 shows the wavelength of the oscillations  $\lambda_{\text{osc}} = 2\pi/w_{\text{osc}}$  as a function of the driving velocity  $v$ . The critical width for oscillations  $L_{\text{osc}}=2b_{\text{osc}}$ , first shown in Fig. 6, was added for completeness, while the experimental data reported in Ref. [9] have been added for comparison. It is clear that the wavelength of oscillations agrees rather well with the experimental data, which confirms the assertion in Ref. [9] that the oscillation wavelength  $\lambda_{\text{osc}}$  seems far less sensitive to the fine details of the temperature field than  $L_{\text{osc}}$ .

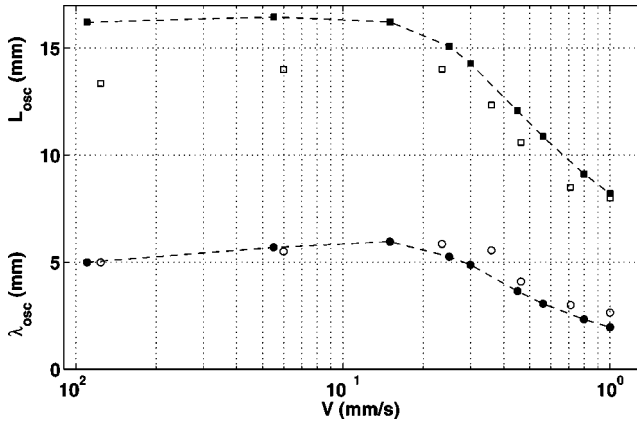


FIG. 7. The wavelength of the oscillations  $\lambda_{\text{osc}} = 2\pi/w_{\text{osc}}$  vs the driving velocity  $v$  for  $\Delta T = 135^\circ\text{C}$  and  $h = 5$  mm. The theoretical values are connected by the dashed lines that were added as guides for the eye. The experimental points that are represented by the unfilled points were extracted from Fig. 15 in Ref. [9]. The results of Fig. 6 were superimposed for completeness. The wavelength of oscillations  $\lambda_{\text{osc}}$  seems far less sensitive to the fine details of the temperature field than  $L_{\text{osc}}$ .

As we have indicated before, there are several relevant length scales in the problem. Here we have calculated a quantity that has the dimension of length and we wanted to explore its dependence on the various length scales in the problem. Therefore, we have calculated the dimensionless oscillation wavelength  $\lambda_{\text{osc}}/L_{\text{osc}}$  at the threshold of instability as a function of the dimensionless thermal diffusion length  $d_{\text{th}}/L_{\text{osc}}$ . The results are shown in Fig. 8. We have found that within the advective regime, which corresponds to relatively high velocities, this function can be well fitted by the linear scaling law  $\lambda_{\text{osc}}/L_{\text{osc}} \approx \alpha + \beta d_{\text{th}}/L_{\text{osc}}$  with  $\alpha = 0.12$  and  $\beta = 2.1$ , to be compared with the experimental

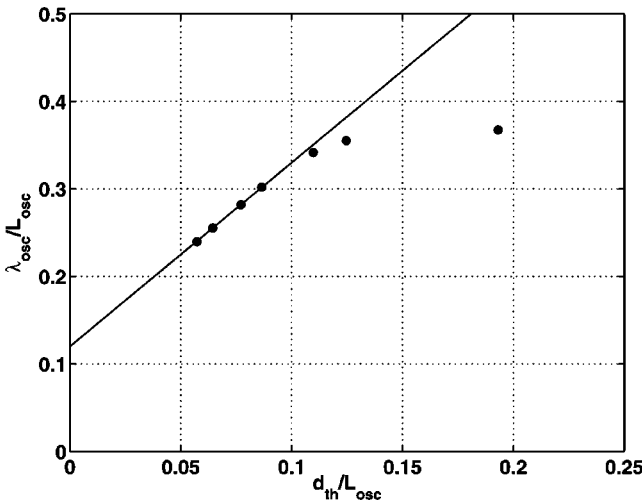


FIG. 8. Dimensionless oscillation wavelength  $\lambda_{\text{osc}}/L_{\text{osc}}$  at the threshold of instability as a function of the dimensionless thermal diffusion length  $d_{\text{th}}/L_{\text{osc}}$ . It is seen that within the advective regime the values can be well fitted by a straight line. This result shows that the scaling between  $\lambda_{\text{osc}}$  and  $L_{\text{osc}}$  is controlled by the thermal diffusion length.

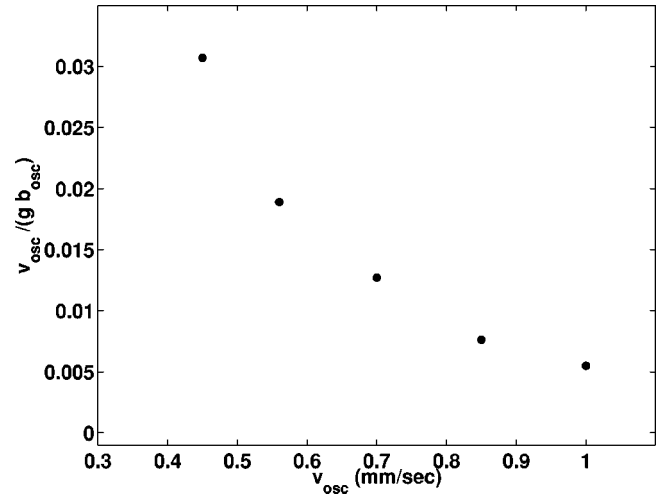


FIG. 9.  $v_{\text{osc}}/(g b_{\text{osc}})$  as a function of  $v_{\text{osc}}$  for velocities in the advective regime, where  $g \equiv f E \alpha_T \Delta T \sqrt{b_{\text{osc}}}$ .

values of  $\alpha = 0.15$  and  $\beta = 2.5$  [9] and the FEM simulation values of  $\alpha = 0.14$  and  $\beta = 2.1$  [17]. This result shows that the scaling between  $\lambda_{\text{osc}}$  and  $L_{\text{osc}}$  is controlled by the thermal diffusion length.

Up to now we have dealt with the matching of the phases of both sides of Eq. (42). The matching of the amplitudes will enable us to calculate the function  $f$ . We stress that calculating  $f$  is not related to the comparison with the experiment which is exhausted by the matching of the phases.

The RHS of Eq. (42), at the critical point, has the form

$$A E \alpha_T \Delta T \sqrt{b_{\text{osc}}} A^* \sin(w_{\text{osc}} v_{\text{osc}} t), \quad (43)$$

where  $A^*$  is a dimensionless amplitude to be calculated. By equating the amplitudes of both sides of Eq. (42) we obtain

$$f = \frac{w_{\text{osc}}^2 v_{\text{osc}}}{E \alpha_T \Delta T \sqrt{b_{\text{osc}}} A^*}. \quad (44)$$

The function  $f$  determines the decay length of perturbations with finite  $K_{\text{II}}$  back to a pure mode I propagation in the straight crack regime. A typical length is constructed from  $v_{\text{osc}}/g$ , where  $g \equiv f E \alpha_T \Delta T \sqrt{b_{\text{osc}}}$ . Figure 9 shows  $v_{\text{osc}}/g$  (in units of  $b_{\text{osc}}$ ) as a function of  $v_{\text{osc}}$  for velocities in the advective regime where the theory agrees with the experiment. It is seen that this length (in units of  $b_{\text{osc}}$ ) decreases as the velocity increases. Assuming that this behavior is not sensitive to the details of the temperature field, it is a challenge to any theory that will suggest an independent derivation of  $f$ . Note that in this calculation  $f$  turns out to be velocity dependent. This is not unreasonable since  $f$  is expected on general grounds to be a function of  $K_{\text{I}}$  and  $K_{\text{II}}^2$  [11]. It is not impossible however that the velocity dependence is an artifact of the ideal baths assumption, similar to the influence on  $\Gamma$  reported in Ref. [7].

### D. The critical exponents of the amplitude of oscillations

In the previous sections we discussed how the solution of the equation of motion changes its nature from an  $A=0$  solution to an  $A \neq 0$  solution, but since we considered all the relevant quantities to  $O(A)$  we could not study the properties of the amplitude itself. In order to extend our analysis we should introduce a time dependent amplitude in our ansatz

$$y(x,t) = A(x+vt)\sin[w(x+vt)] \quad (45)$$

and write the equation of motion to  $O(A^3)$ . The orientation of the tip of the crack is given by

$$\theta(t) = tg^{-1}[y'(x=0,t)] \approx y'(x=0,t) - \frac{y'^3(x=0,t)}{3}, \quad (46)$$

which upon substitution of our ansatz becomes

$$\begin{aligned} \theta(t) &\approx wA(vt)\cos(wvt) + A'(vt)\sin(wvt) \\ &\quad - \frac{1}{3}[wA(vt)\cos(wvt) + A'(vt)\sin(wvt)]^3, \end{aligned} \quad (47)$$

where the prime denotes a derivative with respect to the argument  $vt$ . Because of the symmetry  $A \rightarrow -A$  the next order term in the expansion of  $K_{II}$  in powers of  $A$  is of  $O(A^3)$ . Thus,

$$\begin{aligned} K_{II} &\approx K_{II}^{(1)}\{A(x+vt)\sin[w(x+vt)]\} \\ &\quad + K_{II}^{(3)}\{A(x+vt)\sin[w(x+vt)]\} + O(A^5), \end{aligned} \quad (48)$$

where  $K_{II}^{(1)}\{\cdot\}$  is the functional that was calculated in the Appendix, being of  $O(A)$ .  $K_{II}^{(3)}\{\cdot\}$  is a functional whose derivation is straightforward but very lengthy; we do not present it explicitly here, but note that it yields a term of  $O(A^3)$ .

In order to proceed we assume that our problem exhibits separation of time scales; the amplitude changes on a typical time that is much longer than the period of oscillations. Hence, we can substitute the expressions for  $\theta$  and  $K_{II}$  into the equation of motion, cf. Eq. (33), and operate on both sides of the equation with the operator  $wv/2\pi \int_0^{2\pi/wv} \{\cdot\} \sin(wvt) dt$  to obtain

$$\begin{aligned} &-vw^2A/2 + vw^4A^3/8 - vw^2AA'/2 + vA''/2 - vw^2A^2A''/8 \\ &\quad - 3vA'^2A''/8 \\ &= -\frac{f w v}{2\pi} \int_0^{2\pi/wv} K_{II}^{(1)}\{A(x+vt)\sin[w(x+vt)]\} \\ &\quad \times \sin(wvt) dt - \frac{f w v}{2\pi} \\ &\quad \times \int_0^{2\pi/wv} K_{II}^{(3)}\{A(x+vt)\sin[w(x+vt)]\} \sin(wvt) dt. \end{aligned} \quad (49)$$

This is a highly nontrivial integro-differential equation for the time evolution of the amplitude  $A$ . We expect that after a transient the amplitude saturates to a fixed value. Therefore, we set all the derivatives to zero and the amplitude equation reduces to

$$\begin{aligned} &-vw^2A/2 + vw^4A^3/8 \\ &= -\frac{f w v}{2\pi} \int_0^{2\pi/wv} K_{II}^{(1)}\{A \sin[w(x+vt)]\} \sin(wvt) dt \\ &\quad - \frac{f w v}{2\pi} \int_0^{2\pi/wv} K_{II}^{(3)}\{A \sin[w(x+vt)]\} \sin(wvt) dt. \end{aligned} \quad (50)$$

If we consider one of the control parameters slightly above its critical value, e.g., the velocity, and expand all the terms around the critical point we obtain

$$\begin{aligned} &-w_{osc}^2A/2 - \epsilon_v(w_{osc}^2 + 2v_{osc}w_{osc}\partial_v w_{osc})A/2 + w_{osc}^4A^3/8 \\ &= -fAK_{II}^{(1)}\{A \sin[w_{osc}(x+v_{osc}t)]\}/2v_{osc} \\ &\quad + \alpha(v_{osc})\epsilon_v A + \beta(v_{osc})A^3. \end{aligned}$$

Here  $\epsilon_v \equiv (v - v_{osc}/v_{osc})$  is the critical parameter,  $\alpha(v_{osc})$  is the coefficient of a critical linear term related to  $\partial_v K_{II}^{(1)}\{A \sin[w_{osc}(x+v_{osc}t)]\}$ ,  $\beta(v_{osc})$  is the coefficient of the noncritical cubic term, and we neglected terms of  $O(\epsilon_v A^3)$ . The linear *noncritical* terms cancel out since these are just the equation to  $O(A)$ . Therefore, we are left with

$$\begin{aligned} 0 &= [(w_{osc}^2 + 2v_{osc}w_{osc}\partial_v w_{osc})/2 + \alpha(v_{osc})]\epsilon_v A \\ &\quad + [-w_{osc}^4/8 + \beta(v_{osc})]A^3, \end{aligned} \quad (51)$$

where  $\partial_v w_{osc} > 0$  since as we increase the velocity we increase the energy flow to the crack tip which requires more crack surface created per unit time. The instability is tantamount to a positive linear coefficient. We *assume* that the cubic term leads to saturation. It follows that

$$A = \frac{(w_{osc}^2 + 2v_{osc}w_{osc}\partial_v w_{osc})/2 + \alpha(v_{osc})}{w_{osc}^4/8 - \beta(v_{osc})} \epsilon_v^{1/2}. \quad (52)$$

This result shows that the critical exponent with respect to  $\epsilon_v$  is  $1/2$ , in agreement with the experimental data [8]. A similar calculation can be presented for the dependence of  $A$  on  $\epsilon_{\Delta T} \equiv (\Delta T - \Delta T_{\text{osc}})/\Delta T_{\text{osc}}$ . Such a calculation results in the same exponent  $1/2$  as observed in the experiment.

Two comments are in order. First, we *derived* the amplitude equation from the dynamics of the tip, Eq. (33), rather than guess it as in previous works. More stamina can in principle lead to an actual calculation of the last term in this equation. Second, we have projected the full amplitude equation onto its asymmetric part. Projecting onto the symmetric (cosine) part yields the equation

$$\begin{aligned} & v w A' - v w^3 A^2 A' / 2 - v w A'^3 / 4 - v w A A' A'' / 4 \\ &= - \frac{f w v}{2 \pi} \int_0^{2\pi/wv} K_{\text{II}}^{(1)} \{A(x+vt) \sin[w(x+vt)]\} \\ & \quad \times \cos(wvt) dt - \frac{f w v}{2 \pi} \\ & \quad \times \int_0^{2\pi/wv} K_{\text{II}}^{(3)} \{A(x+vt) \sin[w(x+vt)]\} \cos(wvt) dt. \end{aligned} \quad (53)$$

Discarding again, for the stationary state, all the derivatives, we see that we do not gain any new information about the stationary amplitude. On the other hand, we learn that also the last term is a pure sine function, since it has to vanish at the critical point exactly like the  $K_{\text{II}}^{(1)}$  term.

#### IV. CONCLUDING REMARKS

The main point of departure of our theory from previous ones is that we employ, in addition to the two-dimensional linear elasticity part, the dynamical crack-tip propagation law suggested in Ref. [11]. Using this dynamical law we first derived a stability criterion for the straight crack propagation, which is identical to a previously suggested criterion [4,5]. We then extended the analysis to the evolution of the crack shape just above the onset of the oscillatory instability and showed that the dynamical equation has a stationary sinusoidal solution with a theoretically calculated wave number. We should stress at this point that this trajectory *evolves with  $K_{\text{II}} \neq 0$  except at isolated points*. Thus the ‘‘principle of local symmetry’’ is shown to be insufficient as a dynamical criterion. We presented a quantitative comparison with the experimental data for a temperature field that is characterized both by the spatial separation between the thermal baths  $h$  and the thermal diffusion length  $d_{th}$ . Our results agree rather well with the experiments [9].

From the conceptual point of view we have offered a successful way to decompose the problem into a singular and a nonsingular part. This decomposition enabled us to derive an expression for  $K_{\text{II}}$  to leading order in the amplitude of the oscillations that depended only on the factorization of one Wiener-Hopf kernel. This factorization is done by applying the method of Padé approximants suggested recently [12]. Finally, we showed how the dynamical tip propagation law

translates to an amplitude equation for the oscillatory solution. This equation resulted in calculated critical exponents of the transition, in agreement with the measured ones. The success of the dynamical theory based on the law of tip propagation lends strong support to this law, at least in these quasistatic conditions. One should stress at this point that the analysis considered the temperature field as effectively frozen. The oscillatory nature of the crack has very little to do with the temperature dynamics. This cannot be expected to remain valid for larger amplitudes of oscillations since the boundary condition restricts the temperature level sets to be normal to the crack. Thus at some point the dynamics of the temperature field must enter the discussion, potentially leading to new dynamic instabilities including chaos and disorder.

In fact, the conclusion of this study appears to be that in the quasistatic conditions the assumption of small scale yielding holds, making it sufficient to solve the linear elasticity problem, coupled to a correct law of motion that dictates how the tip propagates. It would be interesting to try to apply this or similar laws to other contexts in which the quasistatic problem can be solved, but where the absence of an accepted propagation law has led to a number of possible evolutions [18,19]. We expect however that in truly dynamical crack propagation new theoretical concepts need to be developed in order to reach a similar level of calculation of experimental observations.

#### ACKNOWLEDGMENTS

We thank Vincent Hakim for proposing the problem to us, suggesting that there is substantial amount of theory to be done. This work was supported in part by the Petroleum Research Fund; the Minerva Foundation, Munich, Germany; and by the European Commission under a TMR grant.

#### APPENDIX: SLIGHTLY CURVED CRACKS

The aim of this appendix is to derive Eqs. (39) and (42). Assume that we have a mode I load  $\sigma_{yy}(x,0)$  on a semi-infinite crack whose tip is at  $x=0$ . Let us first find the normal opening stress  $T_n(x,y(x,t))$  and tangential shearing stress  $T_t(x,y(x,t))$  on any small deviation  $y(x,t)$  from straight crack in terms of  $\sigma_{yy}(x,0)$ . The cartesian components of the stress tensor field are related to polar components according to

$$\begin{aligned} \sigma_{xx} &= \sigma_{rr} \cos^2 \theta + \sigma_{\theta\theta} \sin^2 \theta - \sigma_{r\theta} \sin 2\theta, \\ \sigma_{yy} &= \sigma_{rr} \sin^2 \theta + \sigma_{\theta\theta} \cos^2 \theta + \sigma_{r\theta} \sin 2\theta, \\ \sigma_{xy} &= (\sigma_{rr} - \sigma_{\theta\theta}) \sin(2\theta)/2 + \sigma_{r\theta} \cos 2\theta. \end{aligned} \quad (A1)$$

Here  $\theta$  is the local angle made by the tangent to the crack and the  $x$  axis. These relations can be expanded to first order in  $\theta \approx y'(x,t)$  and then inverted to yield

$$\begin{aligned} T_n(x,y(x,t)) &= \sigma_{\theta\theta}(x,y(x,t)) \\ &= \sigma_{yy}(x,y(x,t)) - 2y'(x,t) \sigma_{xy}(x,y(x,t)), \end{aligned} \quad (A2)$$

$$T_t(x, y(x, t)) = \sigma_{r\theta}(x, y(x, t)) = \sigma_{xy}(x, y(x, t)) + y'(x, t) \\ \times [\sigma_{yy}(x, y(x, t)) - \sigma_{xx}(x, y(x, t))].$$

Expanding the cartesian components to first order in  $y(x, t)$

$$\sigma_{yy}(x, y(x, t)) = \sigma_{yy}(x, 0) + \partial_y \sigma_{yy}(x, 0) y(x, t), \\ \sigma_{xy}(x, y(x, t)) = \sigma_{xy}(x, 0) + \partial_y \sigma_{xy}(x, 0) y(x, t), \quad (\text{A3})$$

and using the relation

$$\partial_y \sigma_{xy}(x, 0) = \partial_y (-\partial_x \partial_y \chi) = -\partial_x \partial_y \partial_y \chi = -\sigma'_{xx}(x, 0), \quad (\text{A4})$$

we end up with

$$T_n(x, y(x, t)) = \sigma_{yy}(x, 0), \\ T_t(x, y(x, t)) = y'(x, t) [\sigma_{yy}(x, 0) - \sigma_{xx}(x, 0)] \\ - y(x, t) \sigma'_{xx}(x, 0), \quad (\text{A5})$$

where we used the symmetry of the problem to set  $\sigma_{xy}(x, 0) = 0$ ;  $\sigma_{xx}(x, 0)$  can be calculated from the knowledge of the boundary condition  $\sigma_{yy}(x, 0)$ .

The problem we should solve now is formulated as follows. Given the following crack configuration and loading conditions: (i) a semi-infinite crack whose shape is described by a small deviation  $y(x, t)$  from a straight crack configuration in an infinite two-dimensional domain (ii) a normal opening load  $T_n(x, y(x, t))$  and a shear load  $T_t(x, y(x, t))$  at any point on the crack, what are the mixed mode stress intensity factors?

A version of this problem was treated completely by Cotterell and Rice [13]. They have found that the stress intensity factors for a finite slightly curved crack extending from  $-a$  to  $a$ , where the deviation vanishes at both tips, are given by

$$K_I - iK_{II} = \frac{1}{\sqrt{\pi a}} \int_{-a}^a dx [q_I(x) - iq_{II}(x)] \sqrt{\frac{a+x}{a-x}}, \quad (\text{A6})$$

where  $q_I(x)$  and  $q_{II}(x)$  were derived explicitly in Ref. [13]. In order to adapt this result to our semi-infinite configuration we should fix one tip of the crack to  $x=0$ , take the limit where the other tip goes to  $-\infty$ , and finally shift the origin,

$$\tilde{y}(x, t) = y(x, t) - y(0, t), \quad (\text{A7})$$

such that the deviation vanishes as the tip of the crack at any time. This adaptation yields

$$K_I - iK_{II} = \sqrt{\frac{2}{\pi}} \int_{-\infty}^0 \frac{dx [q_I(x) - iq_{II}(x)]}{\sqrt{-x}}, \quad (\text{A8})$$

where

$$q_I = T_n - \frac{3}{2} \tilde{y}'(0, t) T_t + \tilde{y}(x, t) T_t' + 2 \tilde{y}(x, t) T_t, \\ q_{II} = T_t + \tilde{y}(x, t) T_n' + \frac{1}{2} \tilde{y}'(0, t) T_n. \quad (\text{A9})$$

Using the derived loading conditions of Eq. (A5) and applying these results to our ansatz for  $y(x, t)$  we obtain

$$q_I = \sigma_{yy}(x, 0) + O(A^2), \\ q_{II} = \{A \sin[w(x+vt)] [\sigma_{yy}(x, 0) - \sigma_{xx}(x, 0)]\}' \\ - A \sin(wvt) \sigma'_{yy}(x, 0) + \frac{1}{2} A w \cos(wvt) \sigma_{yy}(x, 0) \\ + O(A^3). \quad (\text{A10})$$

The last step is to relate  $\sigma_{xx}(x, 0)$  to the boundary condition  $\sigma_{yy}(x, 0)$ . According to the complex potentials method [15] we have for a semi-infinite straight crack

$$\sigma_{yy} + \sigma_{xx} = 4 \operatorname{Re}[\Phi(z)] \quad (\text{A11})$$

with

$$\Phi(z) = \frac{1}{2\pi\sqrt{z}} \int_{-\infty}^0 \frac{dx [\sigma_{yy}(x, 0) - i\sigma_{xy}(x, 0)] \sqrt{-x}}{z-x}. \quad (\text{A12})$$

Since in our case there is no shear loading on the straight crack we obtain

$$q_I = \sigma_{yy}(x, 0) + O(A^2), \quad (\text{A13})$$

$$q_{II} = \{2A \sin[w(x+vt)] \sigma_{yy}(x, 0)\}' - A \sin(wvt) \sigma'_{yy}(x, 0) \\ + \frac{1}{2} A w \cos(wvt) \sigma_{yy}(x, 0) + O(A^3),$$

which becomes, upon substitution into Eq. (A8), the RHS of Eq. (42) and by setting  $t=0$  and integrating by parts gives Eqs. (39).

[1] A. Yuse and M. Sano, Nature (London) **362**, 329 (1993).

[2] J. Fineberg and M. Marder, Phys. Rep. **313**, 1 (1999).

[3] M. Marder, Phys. Rev. E **49**, R51 (1994).

[4] M. Adda-Bedia and Y. Pomeau, Phys. Rev. E **52**, 4105 (1995).

[5] M. Adda-Bedia and M. Ben Amar, Phys. Rev. Lett. **76**, 1497 (1996).

[6] R.V. Gol'dstein and R. Salganik, Int. J. Fract. **10**, 507 (1974).

[7] O. Ronsin, F. Heslot, and B. Perrin, Phys. Rev. Lett. **75**, 2352 (1995).

[8] A. Yuse and M. Sano, Physica D **108**, 365 (1997).

[9] O. Ronsin and B. Perrin, Phys. Rev. E **58**, 7878 (1998).

[10] B. Yang and K. Ravi-Chandar, J. Mech. Phys. Solids **49**, 91 (2001).

[11] J. Hodgdon and J. Sethna, Phys. Rev. B **47**, 4831 (1993).

[12] I.D. Abrahams, IMA J. Appl. Math. **65**, 257 (2000).

- [13] B. Cotterell and J.R. Rice, *Int. J. Fract.* **16**, 155 (1980).
- [14] B. Noble, *Methods Based on the Wiener-Hopf Technique for the Solution of Partial Differential Equations* (Pergamon, New York, 1958).
- [15] N.I. Muskhelishvili, *Some Basic Problems of the Mathematical Theory of Elasticity* (Noordhoff, Groningen, 1953).
- [16] S. Sasa, K. Sekimoto, and H. Nakanishi, *Phys. Rev. E* **50**, R1733 (1994).
- [17] H.A. Bahr, A. Gerbatsch, U. Bahr, and H.J. Weiss, *Phys. Rev. E* **52**, 240 (1995).
- [18] A. Levermann and I. Procaccia, *Phys. Rev. Lett.* **89**, 234501 (2002).
- [19] F. Barra, A. Levermann, and I. Procaccia, *Phys. Rev. E* **66**, 066122 (2002).